High-Q terahertz Fano resonance with extraordinary transmission in concentric ring apertures

Jie Shu,[1] Weilu Gao,[1] Kimberly Reichel,[1] Daniel Nickel,[1] Jason Dominguez,[2] Igal Brener,[2,3] Daniel M. Mittleman,[1] and Qianfan Xu[1,*]

[1]*Department of Electrical and Computer Engineering, Rice University, Houston, TX 77005, USA*
[2]*Sandia National Laboratory, Albuquerque, New Mexico 87185, USA*
[3]*Center for Integrated Nanotechnologies, Sandia National Laboratory, Albuquerque, New Mexico 87185, USA*
[*]*qianfan@rice.edu*

Abstract: We experimentally demonstrate a polarization-independent terahertz Fano resonance with extraordinary transmission when light passes through two concentric subwavelength ring apertures in the metal film. The Fano resonance is enabled by the coupling between a high-Q dark mode and a low-Q bright mode. We find the Q factor of the dark mode ranges from 23 to 40, which is 3~6 times higher than Q of bright mode. We show the Fano resonance can be tuned by varying the geometry and dimension of the structures. We also demonstrate a polarization dependent Fano resonance in a modified structure of concentric ring apertures.

OCIS codes: (310.6628) Subwavelength structures, nanostructures; (260.5740) Resonance; (300.6495) Spectroscopy, terahertz; (120.7000) Transmission.

References and links

1. W. Withayachumnankul, H. Lin, K. Serita, C. M. Shah, S. Sriram, M. Bhaskaran, M. Tonouchi, C. Fumeaux, and D. Abbott, "Sub-diffraction thin-film sensing with planar terahertz metamaterials," Opt. Express **20**(3), 3345–3352 (2012).
2. C. Debus and P. H. Bolivar, "Frequency selective surfaces for high sensitivity terahertz sensing," Appl. Phys. Lett. **91**(18), 184102 (2007).
3. N. Soltani, É. Lheurette, and D. Lippens, "Wood anomaly transmission enhancement in fishnet-based metamaterials at terahertz frequencies," J. Appl. Phys. **112**(12), 124509 (2012).
4. H.-T. Chen, H. Lu, A. K. Azad, R. D. Averitt, A. C. Gossard, S. A. Trugman, J. F. O'Hara, and A. J. Taylor, "Electronic control of extraordinary terahertz transmission through subwavelength metal hole arrays," Opt. Express **16**(11), 7641–7648 (2008).
5. M. Seo, J. Kyoung, H. Park, S. Koo, H. S. Kim, H. Bernien, B. J. Kim, J. H. Choe, Y. H. Ahn, H.-T. Kim, N. Park, Q.-H. Park, K. Ahn, and D. S. Kim, "Active Terahertz Nanoantennas Based on VO2 Phase Transition," Nano Lett. **10**(6), 2064–2068 (2010).
6. E. Hendry, M. J. Lockyear, J. Gómez Rivas, L. Kuipers, and M. Bonn, "Ultrafast optical switching of the THz transmission through metallic subwavelength hole arrays," Phys. Rev. B **75**(23), 235305 (2007).
7. J. Shu, C. Qiu, V. Astley, D. Nickel, D. M. Mittleman, and Q. Xu, "High-contrast terahertz modulator based on extraordinary transmission through a ring aperture," Opt. Express **19**(27), 26666–26671 (2011).
8. R. Singh, I. A. I. Al-Naib, M. Koch, and W. Zhang, "Asymmetric planar terahertz metamaterials," Opt. Express **18**(12), 13044–13050 (2010).
9. V. A. Fedotov, M. Rose, S. L. Prosvirnin, N. Papasimakis, and N. I. Zheludev, "Sharp Trapped-Mode Resonances in Planar Metamaterials with a Broken Structural Symmetry," Phys. Rev. Lett. **99**(14), 147401 (2007).
10. R. Singh, I. A. I. Al-Naib, M. Koch, and W. Zhang, "Sharp Fano resonances in THz metamaterials," Opt. Express **19**(7), 6312–6319 (2011).
11. P. Tassin, L. Zhang, T. Koschny, E. N. Economou, and C. M. Soukoulis, "Low-Loss Metamaterials Based on Classical Electromagnetically Induced Transparency," Phys. Rev. Lett. **102**(5), 053901 (2009).
12. S. Zhang, D. A. Genov, Y. Wang, M. Liu, and X. Zhang, "Plasmon-Induced Transparency in Metamaterials," Phys. Rev. Lett. **101**(4), 047401 (2008).
13. H.-R. Park, Y.-M. Bahk, K. J. Ahn, Q.-H. Park, D.-S. Kim, L. Martín-Moreno, F. J. García-Vidal, and J. Bravo-Abad, "Controlling Terahertz Radiation with Nanoscale Metal Barriers Embedded in Nano Slot Antennas," ACS Nano **5**(10), 8340–8345 (2011).

#202571 - $15.00 USD Received 9 Dec 2013; revised 30 Jan 2014; accepted 31 Jan 2014; published 10 Feb 2014

14. Y.-M. Bahk, J.-W. Choi, J. Kyoung, H.-R. Park, K. J. Ahn, and D.-S. Kim, "Selective enhanced resonances of two asymmetric terahertz nano resonators," Opt. Express **20**(23), 25644–25653 (2012).
15. C. Wu, A. B. Khanikaev, R. Adato, N. Arju, A. A. Yanik, H. Altug, and G. Shvets, "Fano-resonant asymmetric metamaterials for ultrasensitive spectroscopy and identification of molecular monolayers," Nat. Mater. **11**(1), 69–75 (2011).
16. A. Artar, A. A. Yanik, and H. Altug, "Multispectral Plasmon Induced Transparency in Coupled Meta-Atoms," Nano Lett. **11**(4), 1685–1689 (2011).
17. B. Luk'yanchuk, N. I. Zheludev, S. A. Maier, N. J. Halas, P. Nordlander, H. Giessen, and C. T. Chong, "The Fano resonance in plasmonic nanostructures and metamaterials," Nat. Mater. **9**(9), 707–715 (2010).
18. N. Liu, T. Weiss, M. Mesch, L. Langguth, U. Eigenthaler, M. Hirscher, C. Sönnichsen, and H. Giessen, "Planar metamaterial analogue of electromagnetically induced transparency for plasmonic sensing," Nano Lett. **10**(4), 1103–1107 (2010).
19. Y. Zhang, T. Q. Jia, H. M. Zhang, and Z. Z. Xu, "Fano resonances in disk-ring plasmonic nanostructure: strong interaction between bright dipolar and dark multipolar mode," Opt. Lett. **37**(23), 4919–4921 (2012).
20. F. Hao, Y. Sonnefraud, P. Van Dorpe, S. A. Maier, N. J. Halas, and P. Nordlander, "Symmetry Breaking in Plasmonic Nanocavities: Subradiant LSPR Sensing and a Tunable Fano Resonance," Nano Lett. **8**(11), 3983–3988 (2008).
21. N. Papasimakis, Y. H. Fu, V. A. Fedotov, S. L. Prosvirnin, D. P. Tsai, and N. I. Zheludev, "Metamaterial with polarization and direction insensitive resonant transmission response mimicking electromagnetically induced transparency," Appl. Phys. Lett. **94**(21), 211902 (2009).
22. Z.-G. Dong, M.-X. Xu, S.-Y. Lei, H. Liu, T. Li, F.-M. Wang, and S.-N. Zhu, "Negative refraction with magnetic resonance in a metallic double-ring metamaterial," Appl. Phys. Lett. **92**(6), 064101 (2008).
23. S. W. Yu, J. H. Shi, Z. Zhu, R. Liu, and C. Y. Guan, "Multi-peak electromagnetically induced transparency in concentric multiple-ring metamaterials," J. Opt. **15**(7), 075103 (2013).
24. Y. Sonnefraud, N. Verellen, H. Sobhani, G. A. E. Vandenbosch, V. V. Moshchalkov, P. Van Dorpe, P. Nordlander, and S. A. Maier, "Experimental Realization of Subradiant, Superradiant, and Fano Resonances in Ring/Disk Plasmonic Nanocavities," ACS Nano **4**(3), 1664–1670 (2010).
25. J. Kim, R. Soref, and W. R. Buchwald, "Multi-peak electromagnetically induced transparency (EIT)-like transmission from bull's-eye-shaped metamaterial," Opt. Express **18**(17), 17997–18002 (2010).
26. J. Shu, W. Gao, and Q. Xu, "Fano resonance in concentric ring apertures," Opt. Express **21**(9), 11101–11106 (2013).
27. E. Prodan, C. Radloff, N. J. Halas, and P. Nordlander, "A Hybridization Model for the Plasmon Response of Complex Nanostructures," Science **302**(5644), 419–422 (2003).
28. M. A. Ordal, R. J. Bell, R. W. Alexander, Jr., L. L. Long, and M. R. Querry, "Optical properties of fourteen metals in the infrared and far infrared: Al, Co, Cu, Au, Fe, Pb, Mo, Ni, Pd, Pt, Ag, Ti, V, and W," Appl. Opt. **24**(24), 4493–4499 (1985).
29. D. Mittleman, *Sensing with Terahertz Radiation* (Springer, 2003).
30. N. K. Grady, N. J. Halas, and P. Nordlander, "Influence of dielectric function properties on the optical response of plasmon resonant metallic nanoparticles," Chem. Phys. Lett. **399**(1-3), 167–171 (2004).

1. Introduction

Terahertz (THz) on-chip planar metamaterials have emerged as an important active and passive device with different functionalities, such as sensing [1–3], extraordinary transmission [4–7], and asymmetric transmission [8]. In order to enhance light-matter interactions at a very fundamental level, many of the applications require metamaterials that support sharp resonances with high quality factor (Q) associated with high field enhancement. However, it is difficult to reach high Q in planar metamaterials, either in the THz or optical frequency regions. In addition to damping due to the finite conductivity of metals and surface roughness, these structures are usually strongly coupled to free space which causes high radiation losses [9]. Therefore, most THz on-chip resonators suffer from low Q factors, which limits their applications in spectroscopy, biosensing, communications and nonlinear optics. However, the problem of low Q factors in terahertz metamaterials can be tackled if the metamaterial structural design is engineered in such a way that it could support Fano resonances [9,10].

Recent studies have reported Fano resonances in plasmonic nanostructure complexes [9,11–18]. Fano resonances originate from the coupling between a broad bright mode and a narrow dark mode supported in these systems. Fano resonances in metamaterials are realized through symmetry breaking and thus most of them are polarization dependent [9,15,16,19,20]. However, several studies also have reported polarization insensitive Fano resonances in subwavelength concentric metallic rings in radio frequency region [21–23], in

#202571 - $15.00 USD Received 9 Dec 2013; revised 30 Jan 2014; accepted 31 Jan 2014; published 10 Feb 2014

optical and near-infrared spectral ranges [24], and theoretically in THz region [25], or concentric ring apertures in the metal film in mid-infrared (MIR) range [26].

In this paper, we theoretically and experimentally demonstrate a polarization independent Fano resonance in concentric two-ring aperture arrays in a metallic film in the THz spectral range. As we have demonstrated in [26], when two concentric metallic ring apertures are placed close to each other, the near-field coupling between them gives rise to two hybridized modes: a broadband bright mode and a narrowband dark mode [27]. For the bright mode, the E-fields in the two apertures are in-phase, and for the dark mode, the E-fields have opposite phase. Due to the local asymmetry (different radii) between the two ring apertures, the two hybridized modes are not exactly orthogonal to each other. The coupling between the two hybridized modes results in the characteristic Fano line shape in the transmission spectra. Given the symmetry of the structures, the Fano resonance is independent of the polarization of the incident light. For THz concentric 2-ring apertures, the measured Q of the dark mode ranges from 23 to 40, which is much higher than that in MIR concentric two-ring aperture structures [28]. The THz Fano resonance can be tuned by varying geometry and dimension of the structures. We also show that in a modified structure, the Fano resonance can be switched on and off by changing the polarization of incident THz beam, which reveals the different nature of current flow patterns between the bright and dark modes.

2. Fabrication

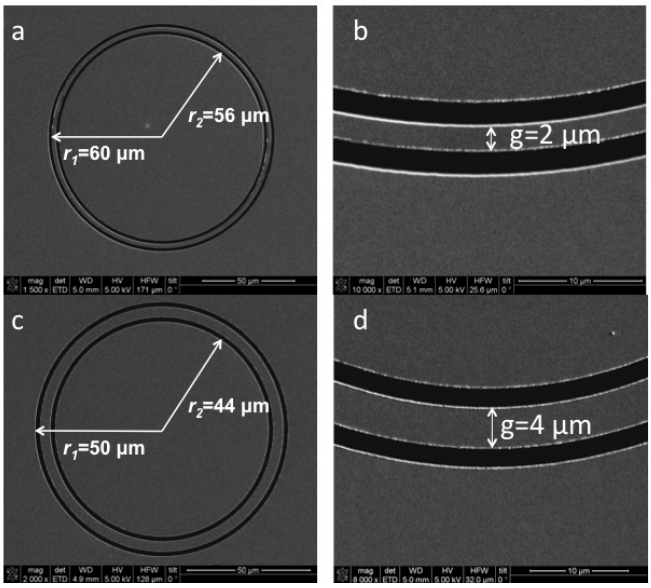

Fig. 1. SEM pictures of fabricated concentric two-ring apertures in the gold film. (a) and (b): r_1 = 60 μm, r_2 = 56 μm, w = 2 μm, g = 2 μm. (c) and (d): r_1 = 50 μm, r_2 = 44 μm, w = 2 μm, g = 4 μm.

Periodic arrays of concentric two-ring apertures in a gold film were fabricated by photo-lithography. The concentric ring patterns were first defined on a 3-μm-thick photoresist AZ 4330 on a 3-mm-thick high resistivity silicon substrate. Then a 500-nm-thick gold film was evaporated with a 20-nm-thick adhesion layer of titanium between the gold film and the silicon substrate, followed by a lift-off process. Figure 1 shows the SEM images of the fabricated devices. The samples consist of arrays of concentric ring apertures fabricated with different radii and gaps, but all with the same aperture width of w = 2 μm and same period of p = 150 μm. The outer radii r_1 of the 2-ring apertures varies from 40 μm to 60 μm, and edge-

#202571 - $15.00 USD Received 9 Dec 2013; revised 30 Jan 2014; accepted 31 Jan 2014; published 10 Feb 2014

to-edge gap g between the two apertures varies from 2 μm to 8 μm. The total size of each array is 2 cm × 2 cm, in order to exceed the size of the incident THz beam.

3. Results

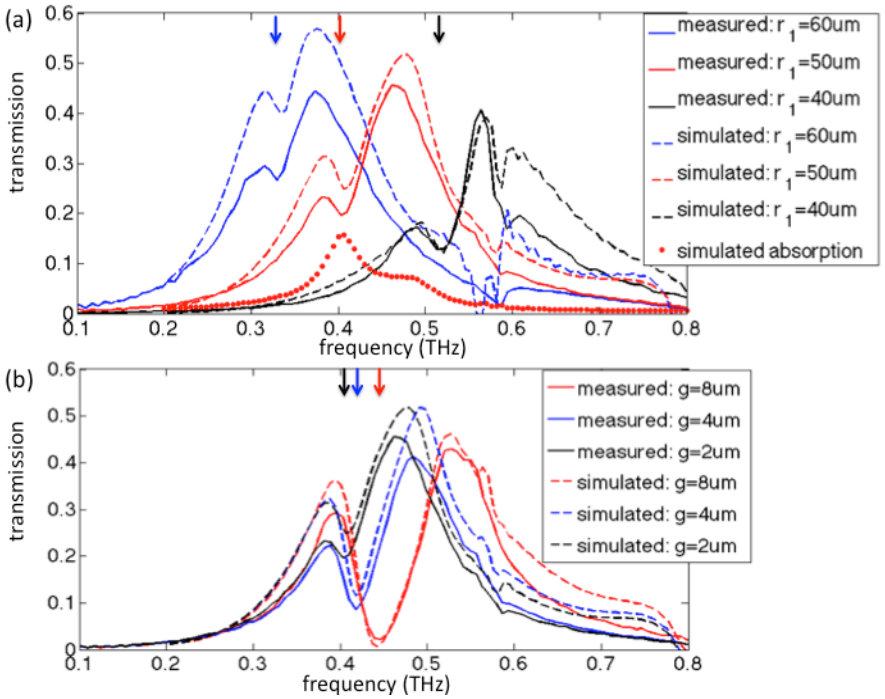

Fig. 2. Measured (solid lines) and simulated (dashed lines) transmission spectra of concentric 2-ring apertures in gold film. Same color stands for same structure for experiment and simulation. The spectra are normalized to the transmission of air. Arrows at the top of the spectra marks the frequency locations of Fano dips. (a) Concentric 2-ring apertures with different radii. (b) Concentric 2-ring apertures with different gaps. Red dotted line in (a) shows simulated absorption spectra of concentric 2-ring apertures with r_1 = 50 μm, g = 2 μm.

We experimentally study the Fano resonance in the concentric two-ring aperture arrays using a time domain terahertz spectrometer. The samples are illuminated at normal incidence in a transmission geometry [29]. The solid lines in Fig. 2(a) and Fig. 2(b) show the measured transmission spectra of two-ring aperture arrays with different radii and gaps. All the spectra are normalized to the transmission of air. Transmission peaks, arising from the extraordinary optical transmission (EOT) effect, occur when the optically bright dipole mode in the structure is coupled to the linearly polarized incident THz wave [7,26]. The peak transmission is limited by the large difference in refractive index between air and silicon on the two sides of the structures, as well as the residual absorption of the substrate. The small features on the spectra at around 0.59 THz are due to the grating effect determined by the periodicity of the array. In addition, some small features are observed due to residual water vapor in the beam path. More prominently, Fano resonance dips can be clearly identified at frequency locations indicated by arrows at the top of the spectra in Fig. 2. From Fig. 2(a) we can see the center frequency of the Fano dip scales inversely to the radius of the ring aperture, and from Fig. 2(b) we can see the Fano dip becomes wider and deeper as the gap between two ring apertures increases.

The simulated transmission spectra (dashed lines in Fig. 2) match well with the experiment. We performed a series of 3D finite-difference-time-domain (FDTD) simulations of a normally-incident broadband THz wave passing through the two-ring aperture in a gold

#202571 - $15.00 USD Received 9 Dec 2013; revised 30 Jan 2014; accepted 31 Jan 2014; published 10 Feb 2014

film on an intrinsic silicon substrate. In the simulations, we set the dimensions and geometry of the structures to be the same as in the experiments. We described the gold film by a Drude model with the plasma and the collision frequencies taken as f_p = 2164 THz and f_c = 11 THz, respectively [28,30]. The simulated transmission spectra follow the same Fano lineshape as in the measurements. The slightly higher transmission peak amplitude in the simulations as compared to the experiment could be due to residual absorption in the substrate, or scattering due to roughness or imperfections in the (relatively thick) lithographically deposited metal film. The red dotted curve in Fig. 2(a) shows the simulated absorption spectra of an array of concentric two-ring apertures with r_1 = 50 μm and g = 2 μm. We notice the absorption peaks at the Fano dip location in the corresponding transmission spectrum, due to energy transferring from the bright mode to the dark mode, which confirms the excitation of the dark mode in the structures.

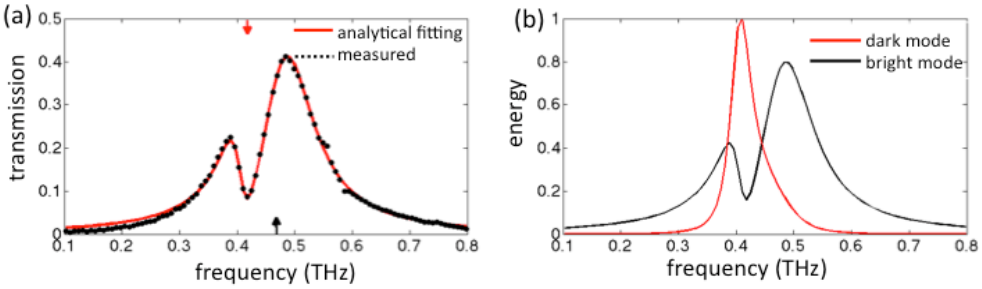

Fig. 3. (a) Measured transmission spectrum (black dotted lines) of the concentric two-ring apertures with r_1 = 50 μm, g = 4 μm can be well fitted by the analytical model (red solid line). The black arrow on the bottom and red arrow on the top indicate the resonant frequency locations of the bright mode and dark mode, respectively. (b) The energy in the dark mode (the red line) and the bright mode (the black line), which are normalized to the maximum energy in the dark mode.

By fitting the measured transmission spectrum with the coupled optical resonator model as described in [26], we can extract information about both the bright mode and the dark mode, including their resonant frequencies, photon lifetimes, and Q factors, and the coupling rate between the two modes. As an example, we show the measured transmission spectrum of the concentric two-ring apertures with r_1 = 50 μm, g = 4 μm, which can be well fitted by the analytical model (Fig. 3(a)). Here, the black arrow on the bottom and red arrow on the top mark the resonant frequencies of the bright mode and dark mode, respectively. We find the bright mode resonating at a frequency of 0.47 THz with a photon lifetime of ~2.39 ps (Q ≈7.03), and the dark mode resonates at a frequency of 0.42 THz with a photon lifetime of ~11.66 ps (Q ≈30.42). The coupling lifetime between the two modes is 0.21 ps^{-1}. The higher Q factor of the dark mode leads to a stronger resonance and higher amplitude of energy stored in the mode, as shown in Fig. 3(b). At the center of the dark mode resonance, the energy in the bright mode reaches close to zero, showing that almost all the optical energy has been transferred from the bright mode to the dark mode, even though the dark mode does not directly couple to the incident THz waves. Using the analytical model, we find as the gap between two ring apertures increases from 2 μm to 8 μm, the Q of the dark mode increases from 23 to 40, while the Q of bright mode keeps the same at the value of 7. This effect can be explained as follows. As the gap increases, it causes larger asymmetry of the local field inside the two ring apertures, which leads to higher coupling rate between the bright and dark modes. Higher coupling rate would increase the optical power transferred from the bright mode to the dark mode, giving broader but wider Fano dips. On the one hand, the extinction ratio of the dark mode resonance would be higher for higher coupling rate; on the other hand, the dark mode resonance would also be broader due to higher coupling loss. Therefore, the full-width half-maximum (inversely proportional to the Q factor) of the dark mode is a

#202571 - $15.00 USD Received 9 Dec 2013; revised 30 Jan 2014; accepted 31 Jan 2014; published 10 Feb 2014

combination of these two effects, which will have a local minimum at a particular gap width with a value greater than g = 8 μm.

4. Selectively disabling dark mode without affecting bright mode

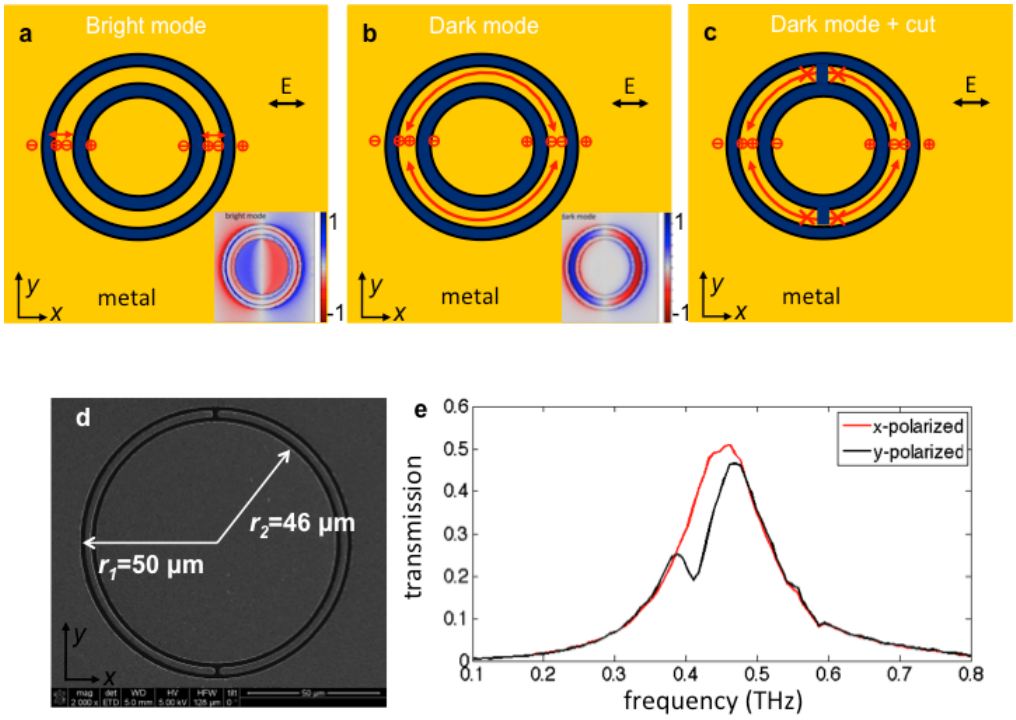

Fig. 4. (a) Scheme of charge motions for the bright mode (a), the dark mode without (b) and with the cut (c) between the apertures. (d) A SEM picture of fabricated concentric two-ring apertures with a cut between the apertures. (e) Measured transmission spectra of concentric two-ring apertures with a cut in the metal between the two apertures, as shown in (d), with different polarization of incident light. The transmission is normalized to the transmission of air. Insets of (a) and (b) show simulated charge distributions of bright mode and dark mode for concentric ring apertures with much smaller dimension.

The Fano resonance in the concentric 2-ring apertures is independent of the polarization of the incident THz beam due to the structural symmetry. With a slight modification of the concentric 2-ring aperture structure as shown in Fig. 4, however, we experimentally demonstrate a polarization dependent Fano resonance, which confirms the different patterns of charge motion (current flow) for the two modes. In the bright mode, the charges in the metal between the two apertures oscillate along the radial direction, as shown in Fig. 4(a). In the dark mode, the charges move along the azimuthal direction as shown in Fig. 4(b), and the current flow is the strongest at the minimum E-field positions (top and bottom portion of the rings). Therefore, if the metal between two ring apertures is cut at the minimum E-field positions as shown in Fig. 4(c), the azimuthal current flow of the dark mode is stopped and the dark mode is suppressed. These cuts have little effect on the bright mode whose radial current flow is not interrupted. As a result, the Fano resonance dip disappears due to the absence of the dark mode while a resonance peak from the bright mode remains (red curve in Fig. 4(e)). When the polarization of the incident wave is rotated 90°, the cuts are now at the maximum E-field location where the azimuthal current flow of the dark mode is zero. Therefore the dark mode is not affected by the cuts and the Fano resonance reappears (black

#202571 - $15.00 USD Received 9 Dec 2013; revised 30 Jan 2014; accepted 31 Jan 2014; published 10 Feb 2014

curve). With this structure, one can selectively turn on and off the Fano resonance and create dramatically different spectra features by changing the polarization of the incident light.

The simulated charge distributions of bright mode and dark mode for concentric ring apertures with a smaller dimension are illustrated as insets in Fig. 4(a) and 4(b), respectively. Typically, we use COMSOL (based on the finite element method in frequency domain) to simulate the charge distribution at a particular frequency. But in the THz frequency range, due to very large difference between the large wavelength and the small scale of the structure, we cannot obtain a meshing in COMSOL that is fine enough to create accurate results and smooth plot. So in order to show the typical charge distribution of different modes, we simulate the same type of concentric ring aperture structure with a smaller dimension than our actual THz structure and thus higher resonant frequency in the mid-infrared range. The simulated structure has same dimension as demonstrated in [26], with radii of r_1 = 950 nm and r_2 = 700 nm, widths of w = 100 nm and an edge-to-edge gap between them of d = 150 nm. The charge distributions for the bright mode (resonating at the center frequency of 982 cm^{-1}) and dark mode (resonating at the center frequency of 827 cm^{-1}) are shown as insets in Fig. 4(a) and 4(b), respectively. We can see the sign of the charge distributions agree with our cartoons in Fig. 4(a) and 4(b).

5. Conclusions

We demonstrate and characterize a THz Fano resonance in subwavelength concentric two-ring apertures in metallic films. This resonance arises from the coupling between a dark mode and a bright mode enabled by the intrinsic asymmetry between the two concentric rings. The measured Q of the dark mode ranges from 23 to 40, with a comparison of Q of bright mode staying same at 7. This indicates a stronger field enhancement for the dark mode as compared to the bright mode, which could be important for application in sensing, spectroscopy, and nonlinear optics. The extraordinary transmission of the two-ring apertures is independent of the polarization of the incident light. In a modified structure, however, we show that the dark mode can be selectively disabled without affecting the bright mode by varying the polarization of the incident light.

Acknowledgments

This work was performed, in part, at the Center for Integrated Nanotechnologies, an Office of Science User Facility operated for the U.S. Department of Energy (DOE) Office of Science. Sandia National Laboratories is a multi-program laboratory managed and operated by Sandia Corporation, a wholly owned subsidiary of Lockheed Martin Corporation, for the U.S. Department of Energy's National Nuclear Security Administration under contract DE-AC04-94AL85000. We also acknowledge partial support from the National Science Foundation (through Grants No. ECCS-1308014 and ECCS-1101171) and the Air Force Office of Scientific Research (AFOSR) Grants FA9550-12-1-0261.

#202571 - $15.00 USD Received 9 Dec 2013; revised 30 Jan 2014; accepted 31 Jan 2014; published 10 Feb 2014